Investigating the Capability of Hyperspectral Imaging for the Estimation of Wheat Leaf Rust Disease

Olivia Crowell, University of Minnesota
September 3, 2016

Abstract

Detecting disease in crops increases yields and reduces economic loss. Traditional methods detect plant disease severity by hand, but it is a slow, time-consuming, and subjective process. Because there are physical, chemical, and physiological changes in plants with diseases, current research focuses on optical imaging as a more useful technique for monitoring disease. This experiment uses hyperspectral imaging (HSI) to investigate its capability as a diagnostic tool for wheat leaf rust disease. HSI has the potential to create more efficient High Throughput Phenotyping (HTP) methods to assist wheat breeders in the selection of a more resistant wheat variety. To collect data for this purpose, a HSI camera was attached to a ground vehicle that scanned wheat plots on an experimental field in St. Paul a month after the fungus was inoculated into the plots. White panels were laid out into the field to normalize the radiance based on the irradiance. Preprocessing techniques converted the pixels from their digital number to reflectance, which measures any physiological changes. The average spectral signatures of pixels were then compared to scoring data on a spectrum of R (resistant) to S (susceptible). Other categories include MR (moderately resistant), MS (moderately susceptible), etc. However, the spectral signatures that matched with R, MR, MRMS, MS, S, etc. varied unreasonably. R and S spectral lines were very similar to each other and did not exist as a maximum and minimum. This study is inconclusive which could be due to the calibration process since light cannot be controlled perfectly. It could also be because of the lack of control with varied wheat during data collection times.

Introduction

Wheat leaf rust is a common disease caused by the *puccinia triticina* fungus, which can decrease wheat yield. It is generally found on wheat leaves during July and August, with symptoms beginning as round yellow spots which eventually turn into orange colored pustules (Ashourloo et al., 2014). These pustules create spores that spread the disease. From 2000 to 2004, wheat yield losses to leaf rust in the USA were estimated at over 3Mt, worth over $350 million (Sharma, 2012). Traditionally, plant disease severity is scored with the visual inspection of plant tissue by trained raters, who categorize disease severity according to a discrete scale (Bock et al., 2010, Mutka et al., 2015). However, this is a subjective technique. It may not be reliable since substantial variation is observed both between individual raters and between different assessments by a single rater (Bock et al., 2008, 2010, Mutka et al., 2015). Therefore, this method of scoring is not considered an accurate method to select the superior line/variety. Additionally, because of the cost of labor and time needed to perform visual assessments of disease, the number of time points from which data can be sampled is limited (Mutka et al., 2015). Overall, this technique is subjective, slow, and costly. As a result, there is an urgent need to develop a method that is rapid, accurate, and non-destructive to help breeders monitor plant traits more precisely and economically. In the past few years, optical imaging and remote sensing techniques have been researched as ways to detect disease for better crop management.

Since plant disease may result in biochemical and structural changes, optical imaging techniques are considered accurate ways of disease identification. The imaging data contains the spectral reflectance values of continuous wave bands of the electromagnetic spectrum, which are influenced by various plant characteristics; any kind of stress causes complex changes in the plants' physiology and composition which, in turn, alters the spectral reflectance pattern (=spectral signature) of plants in the visible range, near infrared, and short-wave infrared (Wahabzada et al., 2016). This technology visualizes data that cannot be seen with the human eye in a non-invasive way. The same organism can be continuously inspected for data over the course of the experiment, and data can be taken at a large scale, making it feasible to study large sample sizes for increased statistical power (Mutka et al., 2015).

This project utilized hyperspectral imaging (HSI) to detect wheat leaf rust since the disease's effect on pigments and structure can be read with the technology. Previous studies have taken place in a lab setting, and this experiment will test the ability of HSI on an outdoor St. Paul field using a ground vehicle as a tool. It will also compare imaging data with ground-truthing to improve image analysis so that the most significant data can be extracted. The objective of this research is to create more efficient High Throughput Phenotyping (HTP) methods in order to assist wheat breeders in the selection of the best wheat variety which is adapted to resist rust disease. I hypothesize that biochemical, structural, and physiological characteristics of wheat leaves attribute to its spectral response.

- <u>Literature Review</u>

There are several optical imaging techniques that assist with HTP methods:

- **Visible light imaging** is intended to mimic human perception to provide information or input to systems. Its silicon sensors (CCD or CMOS arrays) are sensitive to visible bands of light (400–750 nm) and allow imaging in two dimensions. Typically, the raw data of an image is presented in spatial matrices of intensity values corresponding to photon fluxes in the red (~600 nm), green (~550 nm), and blue (~450 nm) spectral bands of visible light (Li et al., 2014).

- **Thermal imaging** is based on the principle that all objects at temperatures above absolute zero (Celsius degree) emit thermal radiation. Intensity and peak wavelength of such radiation varies with the temperature of objects. The thermal portion of the electromagnetic spectrum goes from 7µm-18µm (Campbell et al., 2011).

- **Near infrared imaging** is based on radiation in the near infrared region behaves with respect to optical systems in a manner analogous to radiation in the visible spectrum. Therefore, remote sensing in the near infrared region can use films, filters, and cameras with designs similar to those intended for use with visible light. This region of spectrum extends from 720 nm to 1300 nm (Campbell et al., 2011).

- **Hyperspectral imaging** is a relatively new technology that involves the acquisition of electromagnetic spectra at every pixel in an image, thus combining spatial and spectral information (Bock et al., 2010, Mutka et al., 2015). HSI is represented as a data cube with spatial information collected in the X-Y plane and spectral information represented in the Z-direction. HSI technique is based on both spectroscopy and digital camera technology. Each pixel in a hyperspectral image has its own spectrum, which is a signature that can be assessed for chemical and physical properties. Since each spectrum in a pixel is influenced by its neighboring pixels resulting from various undesired effects such as inhomogeneous samples, environmental changes, and instrumental variations, demolishing methods are available to remove or eliminate any irrelevant information that cannot be minimized or dealt with by regression or classification approaches (Huang et al., 2014). Hyperspectral data sets are generally composed of about 100 to 200 spectral bands of relatively narrow bandwidths (5-10 nm), whereas, multispectral data sets are usually composed of about 5 to 10 bands of relatively large bandwidths (70-400 nm) ("Hyperspectral Remote Sensing", n.d.).

Materials and Methods

- Field Trials:

On the experimental field D-1 in St. Paul, seventy-five plots of different wheat varieties were planted. Every plot in the field consisted of four columns, and each column was broken into eight, five-foot rows. While a single plant genome existed within each five-foot row, the type of genome present within each five-foot row varied from one another. For the purpose of identification, the five-foot rows were each given a unique number. Also included in the wheat plots were spreader rows, which consisted of winter wheat (ww). The configuration of one of these plots is shown in *figure 1,* and the overall plots for the experiment is shown in *figure 2.*

D-1: Section AY1

8	**Ww**	**Ww**	**Ww**	**ww**
7	**Ww**	1043	1044	1045
6	**Ww**	1042	1041	1040
5	**Ww**	1029	1030	1031
4	**Ww**	1028	1027	1026
3	**Ww**	1015	1016	1017
2	**Ww**	1014	1013	1012
1	**Ww**	1001	1002	1003
	1	**2**	**3**	**4**

Figure 1: The first plot of the D-1 field in St. Paul. Only the highlighted rows were considered in the project.

AY1	AY3	AY5	AY7	Scab2	URSN	PYs
	AY2	AY4	AY6	Scab1	URN	

D-1 Field

Figure 2: The overall grouping of the plots for the experiment. *Figure 1* is the first plot of AY1. This research focused on AY1, 2, 4, 6, Scab1, URN, and PYs.

During early June, the winter wheat plants were inoculated with the wheat leaf rust fungus, *Puccinia triticina*. These spreader rows were inoculated a total of three times and by mid-June, they showed signs of rust pustules. As all the wheat grew, the fungi proliferated freely from the winter wheat to the other wheat varieties.

- <u>Data Collection:</u>

On July 18, 2016, a Resonon Pika II hyperspectral imaging camera was attached to a ground vehicle with a distance of 3.3 meters between the lens and plant canopy. *Table 1* lists the camera's properties, and the ground vehicle with the camera are shown together in *figure 3*:

Table 1: Pika II Camera Specifications	
Spectral range	400 – 900 nm
Spectral resolution	2.1 nm
Spatial resolution	3 mm
Spectral channels	240
Spatial channels	640
Max frame rate	145 fps

Figure 3: The camera is attached to a long arm protruding from the ground vehicle. It is collecting hyperspectral images from the wheat field.

The camera uses GPS to trigger its on and off mechanism. A polygon area, shown in *figure 4,* was drawn using google earth, and the camera needs this polygon to know when to start or stop. It will start collecting data as it enters the polygon and it will stop when it leaves the polygon.

Figure 4: The polygon drawn in google earth that triggers the camera's on/off mechanism.

On board the ground vehicle was the flight computer, which is the processor of the incoming data. The computer connected to the GPS, and the camera connected to the computer via an Ethernet cable. It saves the images on an external hard drive.

Imaging occurred around the time of 11:00 AM to 2:00 PM in order to minimize the sun's angle of incidence and shadows. To normalize the radiance based on the irradiance, a white panel was used for calibration. The white panel acted as the highest reflectance possible in the picture, so the rest of the image's pixels contained a spectrum lower than this reflectance. Changes in sunlight affects the reflectance properties of the pixels if the pixels aren't calibrated to the nearest panels.

In collaboration with hyperspectral imaging, ground-truthers went to the fields four to six days before imaging collection in order to score the disease severity. Leaf rust is scored using two data points: a numerical percent of severity (depicted in *figure 5*), and a characterization of resistance (shown in *figure 6*). The two extremes are labeled R, which is resistant and lacks rust, and S, which is susceptible to the fungus. In between variations in include MR (moderately resistant), MS (moderately susceptible), etc. The scorers assigned a label for every unique wheat plot.

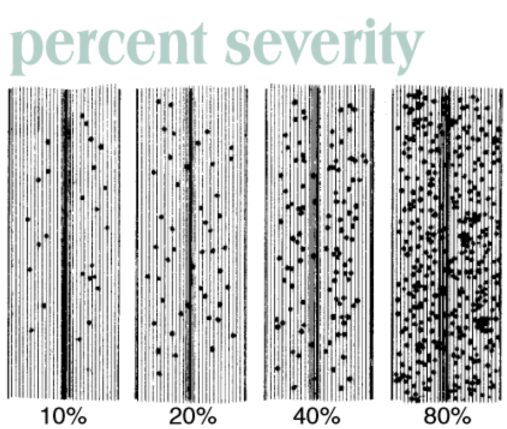

Figure 5. Percent severity. (NDSU graphic)

Figure 6. Wheat leaf rust reaction types. (NDSU photo)

Results

- Data Pre-processing

Figure 7: Raw data from the hyperspectral imaging.

Once the wheat varieties in the images were identified according to their unique number, the program Spectronon was used to convert the raw data as seen in *figure 7* to reflectance. The purpose of this technique was to calibrate the spectral response of the pixels based on the panels. Since disease is detected from changes in the composition of the plant, reflectance is used to measure this property. Within the program, the pixels each had a digital number that was first converted into radiance. *Figure 8* and *Figure 9* show a change in the pixel's spectrum.

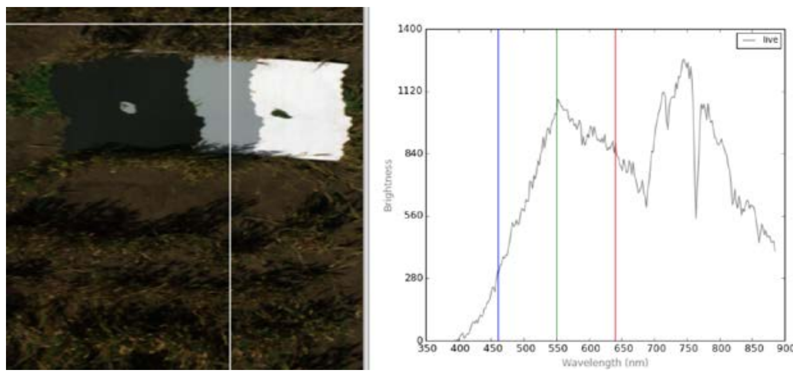

Figure 8: A raw data pixel and its spectrum.

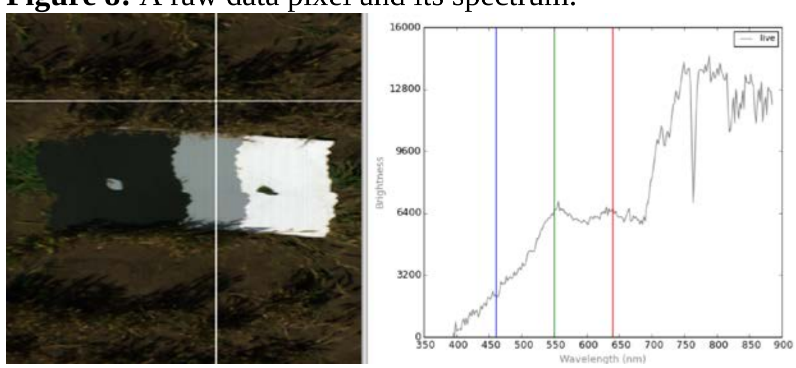

Figure 9: The same pixel in radiance and its new spectrum.

Using the mean spectrum (*figure 10*) of the white panel, the pixels were converted to reflectance (*figure 11*). That enabled the spectral signature of the pixels to meet between 0 and 1 where the white panel created the highest reflectance.

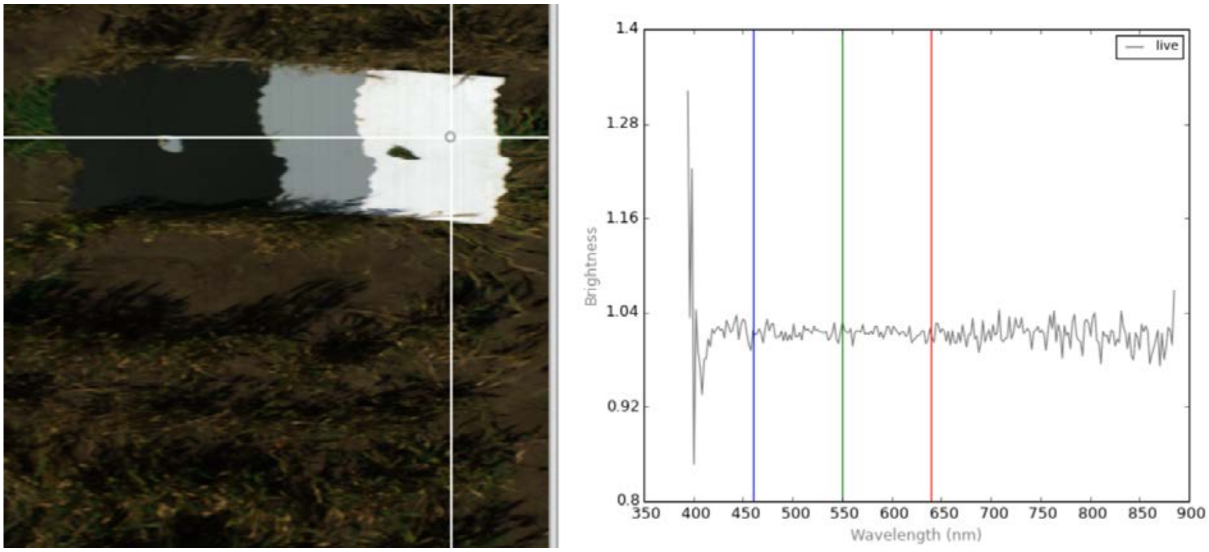

Figure 10: The mean spectrum of the white panel averaging around 1.

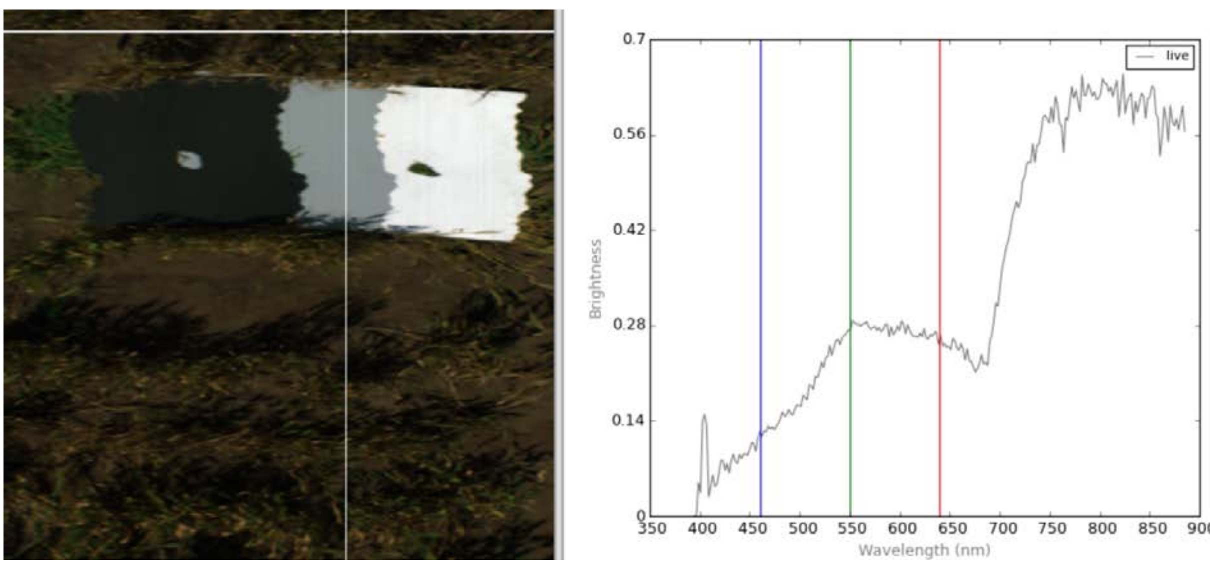

Figure 11: The same pixel in reflectance and its new spectrum.

- <u>Data Analysis</u>

Pixels of the wheat were sorted from the pixels of other entities such as soil and non-wheat plants. Since the vegetative wheat pixels had a general spectral signature that was different from the non-wheat entities, a threshold was placed over the images. Coded in Matlab, the threshold sought wavelengths over a minimum that would exclude soil as well as wavelengths under a maximum that would exclude non-wheat plants. Every row was analyzed individually within this threshold and the spectral signatures of the rows were recorded between 400 to 900 nm.

When every row of wheat with a unique number had a spectral signature and was assigned a score label between R (resistant) or S (susceptible), the two pieces of data were compared. Every spectral signature per unique wheat plot that also was assigned an R category was averaged together so that one spectral signature out of the entire data set would represent R. The same method was carried out with the RMR, MR, MRMS, MSS, and S categories. These lines were compared and analyzed for any differences across the spectrum of R to S, which is depicted in *graph 1*:

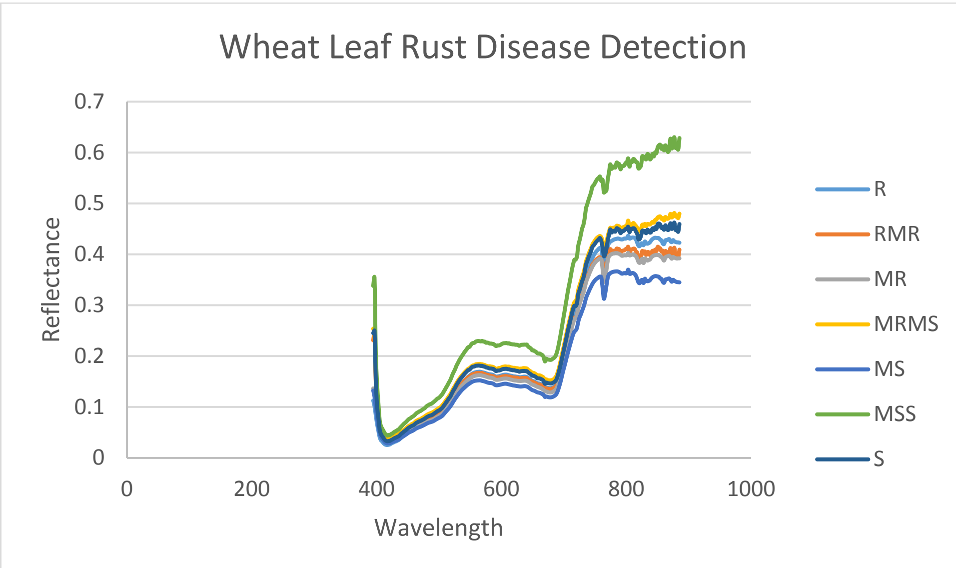

Graph 1: A comparison of the different spectral signatures.

In the figure, a different spectral signature made the labels such as R and MRMS distinct from one another. However, the spectral signatures should have increased in a particular order. Since R and S were on two ends of the spectrum, the R line should have been opposite to the S line. The rest should have filled the spectrum as follows: R, RMR, MR, MRMS, MS, MSS, and S. This was not the case in the overall graph.

An analysis the average spectrums for one frame is shown in *Graph 2*:

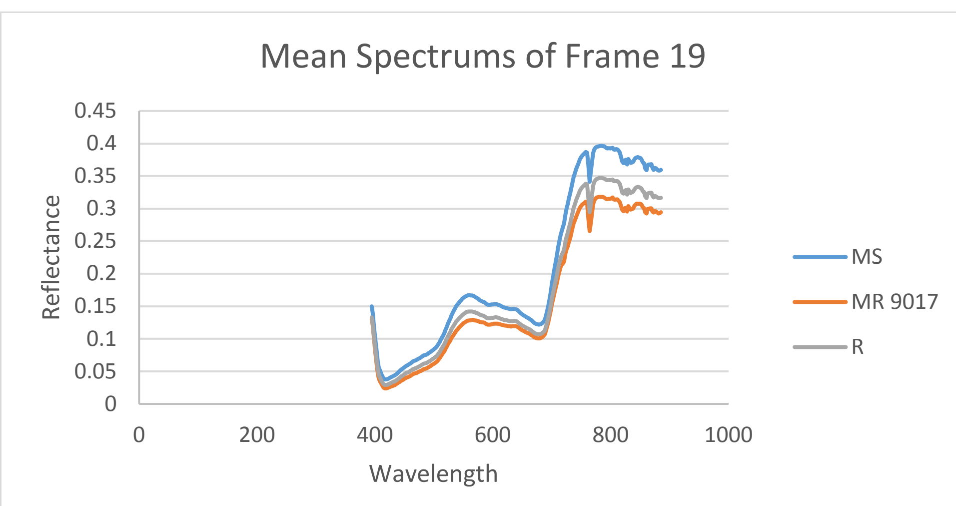

Graph 2: The spectral signatures that exist only in frame 19.

Shown above, there is no reasonable order to R, MR, or MS, which were the only categories that pertained to the wheat in the image. Although a white panel wasn't always in the hyperspectral image, the fact that different frames were calibrated with the nearest panel didn't contribute to the unreasonable order of the spectral signatures.

Conclusion

The study may have been inconclusive for two reasons. Firstly, a flaw could have existed with the calibration of the raw data to reflectance. Since white panels reflect the most light, these panels have the highest reflectance. However, sunlight varies slightly between the panels, which means that the highest reflectance value varies as well. While it is a strong control factor, it is not a perfect control factor. Light changes a lot if the sun's angle of incidence changes or it passes through a cloud. Another reason might be that the study didn't control the wheat genome. A solution to this problem would be to take a control image before the wheat was infected. However, in order for a control image to be taken before inoculation, the control would need to have been taken a month earlier. The distance between the camera lens and the wheat plots would have varied and therefore, it doesn't act as a great control factor for reflectance. Another method to improve the experiment would be to compare spectral signatures within a single plant genome. This is because different plant genomes could be affected with leaf rust differently.

A future study would benefit from having more data collected than just from a couple of rows. Although more rows existed, the computer had trouble connecting to the GPS and couldn't collect data in the time allotted. Also, the day that the raters scored for disease severity should have been closer to the day that the hyperspectral images were taken in order to eliminate any unnecessary error. There also should have been multiple times that the wheat was scored, especially since scoring by hand is a subjective process. The study would have benefitted from having multiple individual raters as well. To accommodate the reflectance variance, panels should also have been more plentiful in the hyperspectral images. As for data analysis, other software such as Envi could have been explored and different probabilistic models created.
By fixing these minor issues, the study could have had a more reasonable spectrum between R and S spectral signatures.

Works Cited

Ashourloo, Davoud, Mohammad Mobasheri, and Alfredo Huete. "Developing Two Spectral Disease Indices for Detection of Wheat Leaf Rust (Pucciniatriticina)." Remote Sensing 6.6 (2014): 4723-740. Web

Bock C. H., Poole G. H., Parker P. E., Gottwald T. R. (2010). Plant disease severity estimated visually, by digital photography and image analysis, and by hyperspectral imaging. Crit. Rev. Plant Sci. 29, 59–107 10.1080/07352681003617285 [Cross Ref]

Campbell, J. B., & Wynne, R. H. (2011). *Introduction to Remote Sensing*. Guilford Press.

Huang, Hui, Li Liu, and Michael Ngadi. "Recent Developments in Hyperspectral Imaging for Assessment of Food Quality and Safety." Sensors 14.4 (2014): 7248-276. Web

"Hyperspectral Remote Sensing." University of Texas, n.d. Web. <http://www.csr.utexas.edu/projects/rs/hrs/hyper.html>

Li, Lei, Qin Zhang, and Danfeng Huang. "A Review of Imaging Techniques for Plant Phenotyping." Sensors 14.11 (2014): 20078-0111. Web

Mutka, Andrew M., and Rebecca S. Bart. "Image-based Phenotyping of Plant Disease Symptoms." Frontiers in Plant Science Front. Plant Sci. 5 (2015): n. pag. Web

Sharma, Indu. "Wheat Leaf Rust." Disease Resistance in Wheat. Wallingford, Oxfordshire: CABI, 2012. 34. Print

Wahabzada, Mirwaes, Anne-Katrin Mahlein, Christian Bauckhage, Ulrike Steiner, Erich-Christian Oerke, and Kristian Kersting. "Plant Phenotyping Using Probabilistic Topic Models: Uncovering the Hyperspectral Language of Plants." Sci. Rep. Scientific Reports 6 (2016): 22482. Web